Civil Engineering Dimension
https://ced.petra.ac.id

Performance Optimization of Strengthened Slab-on-Pile Structure with Braced Frame

Hidayat, M.F.[1], Awaludin, A.[1]*, and Supriyadi, B.[1]
[1] Department of Civil and Environmental Engineering, Gadjah Mada University
Jl. Grafika Kampus No.2, Senolowo, Sinduadi, Mlati, Sleman, Yogyakarta 55284, INDONESIA

DOI: https://doi.org/10.9744/ced.26.2.138-150

Article Info:
Submitted: Dec 25, 2023
Reviewed: Feb 22, 2024
Accepted: Aug 02, 2024

Keywords:
efficiency,
braced frames,
numerical model,
cyclic analysis,
energy dissipation.

Corresponding Author:
Awaludin, A.
Department of Civil and Environmental Engineering, Gadjah Mada University
Jl. Grafika Kampus No.2, Senolowo, Sinduadi, Mlati, Sleman, Yogyakarta 55284, INDONESIA
Email: ali.awaludin@ugm.ac.id

Abstract

Slab-on-pile (SOP) have been constructed widely in many highway projects in Indonesia as it is preferable in soft-soil sites. This study is aimed to determine the optimal structural configuration by adding braced frame devices to the longitudinal direction of the slab-on-pile structure. The optimization process was carried out to obtain the minimum number of pile configurations, reducing construction costs. A total of three numerical models were compared, namely SOP-A, SOP-B, and SOP-C, representing SOP with configurations of 50 piles, 35 piles, and 35 piles plus thirty braced frames, respectively. The cyclic analysis procedure and structure design were executed based on ACI 374.1 and the Indonesian standard SNI 1725:2016. The results showed that all P-M responses of the SOP-A and SOP-C structures met the cross-section capacity requirements, except for the SOP-B. The addition of braced frames in SOP-C facilitated a 38% energy dissipation improvement and caused a significant reduction of number of the spun piles.

Introduction

Slab-on-pile (SOP) is a popular infrastructure method in Indonesia due to its simple structural configuration and fast construction method [1]. A typical configuration of an SOP structure consists of spun piles (pre-stressed hollow concrete), pile heads, and concrete slabs arranged segmentally in the longitudinal direction [2]. Generally, pre-stressed hollow concrete pile is used directly as the piers of SOP structure. Some advantages of using these spun piles include effective erection in soft soil sites, good material durability due to fabrication, and economical cost [3,4].

The application of SOP has been widespread in various Indonesian projects, including the Balikpapan-Samarinda Toll Road, Adi Soemarmo Airport Railway, and Semarang-Demak Toll Road. Typically, SOP are designed with a segmental spacing of five meters and a configuration of five spun piles per pile head. Although designs with longer segmental spacing can reduce time and cost [5], careful consideration of structural performance is essential. Optimization is also important in designing optimal SOP structures to maximize efficiency in terms of time, cost, and structural performance [6,7].

Steel is one of the most common structural building material. In steel structures, braced frames are commonly used in lateral load-resisting systems [8]. This widespread application is attributed to the increased stiffness of braced frames [9,10]. Steel is also characterized by resistance to tensile and compressive forces simultaneously, with good stiffness in the occurrence of earthquakes [11,12]. Braced frames can be applied to SOP to optimize structural performance for easy installation, maintenance, and cost-effectiveness [13].

Note : Discussion is expected before November, 1st 2024, and will be published in the "Civil Engineering Dimension", volume 27, number 1, March 2025.
ISSN : 1410-9530 print / 1979-570X online
Published by : **Petra Christian University**

Based on the background above, this study aimed to determine the optimal structural configuration by adding brace frames in the longitudinal direction of the SOP structure. The optimization process was carried out to obtain the minimum number of spun pile configurations, thereby reducing construction costs. The SOP structures were simulated numerically to obtain a configuration that complies with bridge loading standards according to the Indonesian standard SNI 1725:2016 [14]. Meanwhile, the cyclic analysis method used to determine structural performance and structural energy dissipation follows ACI 374.1 [15]. The results are expected to contribute to the design of cost-effective SOP structures.

Method

Design of the Structures

This study used data from the detailed engineering design (DED) of the Kayu Agung- Palembang-Betung Toll Road project, Pemulutan Regency, South Sumatra Province, Indonesia. The SOP structures were designed following the Indonesian standard SNI 1725:2016, while the cyclic analysis procedure followed ACI 374.1-05. The response modification factor value is 1.5 for the "critical" bridge category [16]. A total of three numerical models were compared, namely SOP-A, SOP-B, and SOP-C (Figure 1). SOP-A is a slab-on-pile with a configuration of 50-spun pile and a spacing of 5 meters. SOP-B serves as a slab-on-pile with a 35-spun pile configuration and a spacing of 7.5 meters. Meanwhile, SOP-C is a slab-on-pile with a configuration of 35-spun pile plus 30 braced frames and a spacing of 7.5 meters. The total longitudinal span of the SOP structure reaches 45 meters, as shown in Figure 2. The modeling procedure was performed using STKO version (OpenSees) 3.3.0 software.

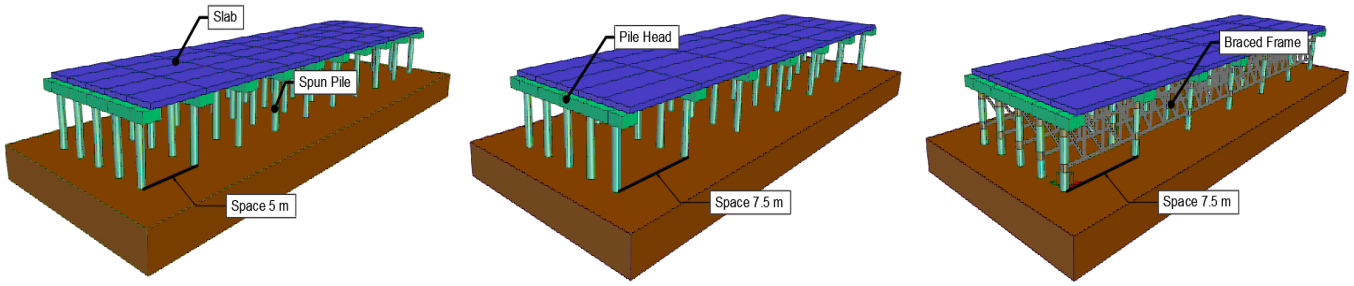

Figure 1. Models Design: (a) SOP-A; (b) SOP-B; (c) SOP-C

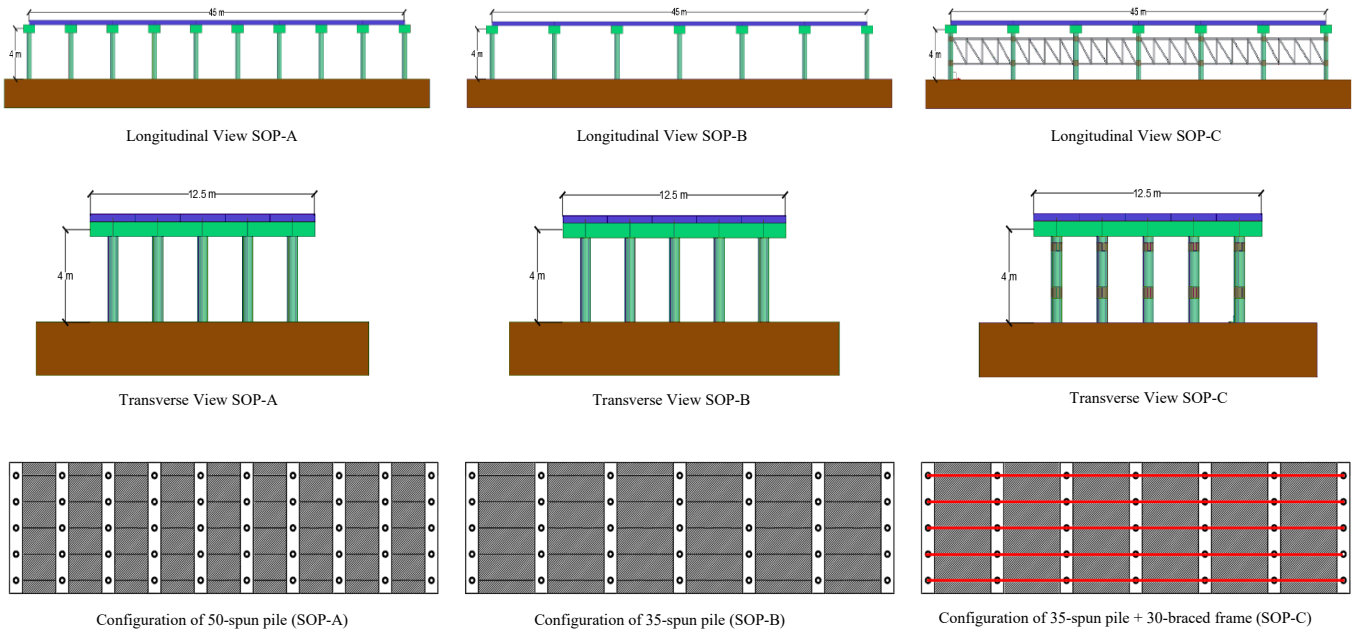

Figure 2. An Overview of the Slab-on-pile Models

Properties of Structures

In this study, the SOP consists of pile heads, slabs, spun piles, and braced frames. Section properties of the SOP and detail of the braced frame are shown in Figure 3 and Figure 4. Each material is modeled as elastic except, for spun

pile which is inelastic because this study only focuses on the non-linear behavior of the spun pile which is the foundation of the slab-on-pile structure. Material details as shown in Table 1 and Table 2.

Table 1. Material Properties of Pile Head, Slab, dan Braced Frame

Elastic Beam Column	Young's modulus, E (MPa)	Shear Modulus, G (MPa)
Pile Head	25742.96	10726.23
Slab	30459.48	12691.45
Steel Braced Frame	200000.0	76923.08

Table 2. Material Properties of Spun Pile

Concrete		PC bar	
f'_c (MPa)	-60	f_y (MPa)	1387
e_{psc0}	-0.002	E (MPa)	220267
f_{pcu} (MPa)	-12	b	0.019
e_{psu}	-0.0053	ε_{min}	-0.018
λ	0.071	ε_{max}	0.018
f_t (MPa)	4.648		
E_{ts} (MPa)	2938		
b" (mm)	327		
s (mm)	100		
p"	0.001		

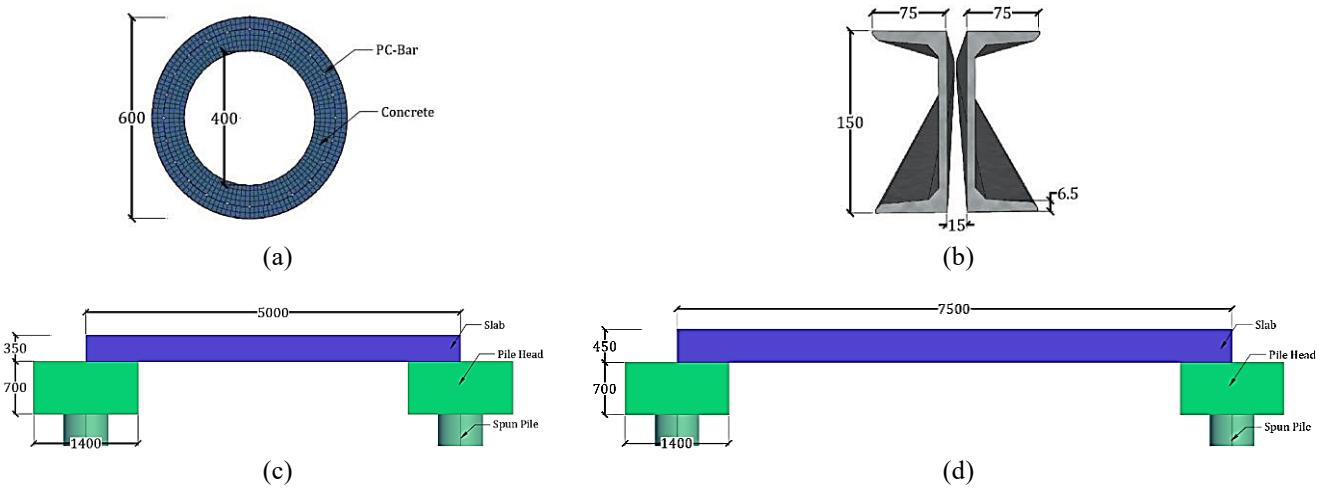

Figure 3. Section Properties: (a) Spun Pile; (b) Double UNP; (c) Detail SOP Span 5000 mm; (d) Detail SOP Span 7500 mm. (unit in mm)

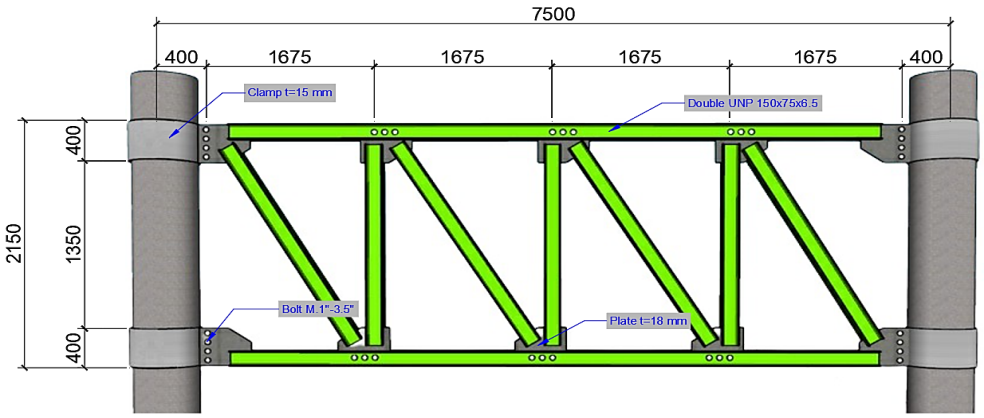

Figure 4. Detail Braced Frame (unit in mm)

Material Model of Concrete and PC Bar

Reinforced concrete structures consist of concrete cover and core, which are located outside and inside the stirrup or spiral, respectively. The presence of stirrups or spirals serves to bond the concrete core and give different properties

between the concrete core and the concrete cover.

Several theories of compressive concrete material models have been developed, including Kent & Park [17], with stress-strain curves presented in Figure 5. The stress-strain relationship is the same to approximately the maximum concrete compressive strength (f'_c). After the maximum concrete compressive strength is exceeded, unconfined concrete experiences rapid deterioration. This is due to the restraining effect of stirrups or spirals that can minimize the escape of confined concrete material. Subsequently, the compressive strength of concrete continues to decrease to its ultimate compressive strength ($0.2\ f'_c$). Other parameters that determine the stress-strain curve of concrete materials are the width or diameter of the concrete core (b"), the spacing between spirals (s), and the volume of spirals to that of the concrete core ratio (p").

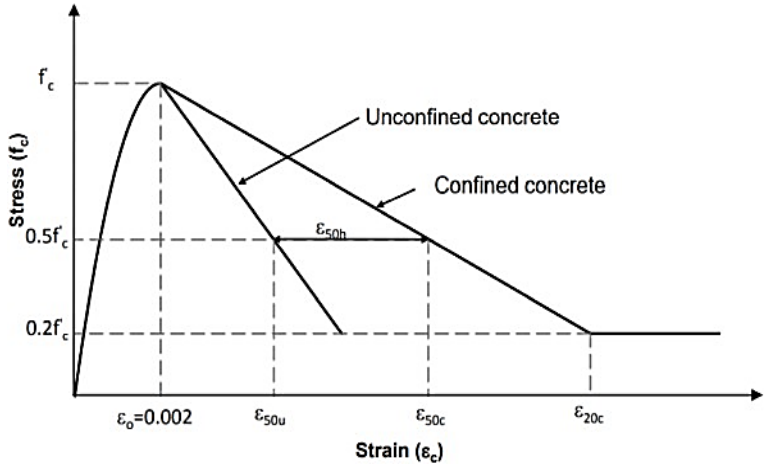

Figure 5. Concrete Stress-strain Curve by Kent and Park [17]

$$f_c = f'_c\left[\frac{2\varepsilon_c}{0.002} - \left(\frac{\varepsilon_c}{0.002}\right)^2\right] for\ \varepsilon_c \leq 0.002 \quad (1)$$

$$f_c = f'_c[1 - Z(\varepsilon_c - 0.002)]\ for\ \varepsilon_c > 0.002 \quad (2)$$

$$Z = \frac{0.5}{\varepsilon_{50u} - 0.002}\ for\ unconfined\ concrete \quad (3)$$

$$Z = \frac{0.5}{\varepsilon_{50h} + \varepsilon_{50u} - 0.002}\ for\ confined\ concrete \quad (4)$$

$$\varepsilon_{50u} = \frac{3 + 0.29 f'_c}{145 f'_c - 1000} \quad (5)$$

$$\varepsilon_{50h} = \frac{3}{4} p'' \sqrt{\frac{b''}{s}} \quad (6)$$

In additional to the compressive strength, the tensile strength of concrete also needs to be considered in modeling concrete materials. The amount of strain and tensile strength of concrete according to Quayyum [18] is determined by the compressive strength of concrete (f'_c) and the initial modulus of concrete (E_0).

$$f_{ct} = 0.6\sqrt{f'_c} \quad (7)$$

$$\varepsilon_{ct} = \frac{f_{ct}}{E_0} \quad (8)$$

$$E_0 = \frac{2 f'_c}{\varepsilon_0} \quad (9)$$

These concrete material models can be combined to produce a complete concrete material model. One program that adopts such a model is the Scientific Tool Kit for OpenSees (STKO) program. In the program, one of the concrete material models that can be used is the *Concrete02* model [19]. In this study, the restrained concrete material model used for spun pile, the parameters determined include concrete compressive strength (f'_c), concrete strain at maximum compressive strength (e_{psc0}), crushing strength (f_{pcu}), strain at crushing strength (e_{psu}), demolition slope ratio from the initial slope (λ), tensile strength (f_t), and stress softening strength (E_{ts}). The PC bar material is described as a bilinear material with a certain strain limit. The parameters considered include yield strength (f_y),

strain hardening ratio (b), initial elastic tangent (E), strain at maximum tensile strength (ε_{max}), and strain at maximum compressive strength (ε_{min}). Moreover, the parameters of concrete and PC bar are modeled in Figure 6. The material parameters of PC bar referred to the experiments conducted by Irawan et.al. [20], which were validated by checking the concrete strain after the analysis was performed.

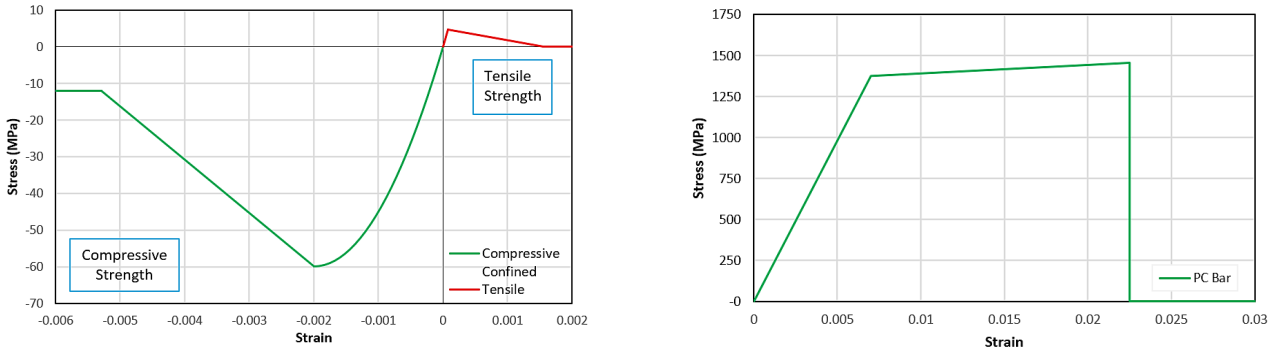

(a) (b)

Figure 6. The Curve of Stress-strain Model of Spun Pile: (a) Concrete and (b) PC Bar

Fixity Depth of Spun Pile Idealization

An initial analysis was performed using STKO (OpenSees) software to streamline the structural model. In this preliminary analysis, all piles were supported by nonlinear soil springs along the embedded section, with a length of 4000 mm in the free head section and 40,000 mm in the embedded section. Soil data were obtained from borhole tests at the project site. The nonlinear soil springs accounted for tip resistance, axial resistance, and horizontal resistance. Based on the numerical analysis results in Figure 7, the fixity point, which experienced the maximum bending moment, was located at a depth of 5000 mm below the ground surface. In the structural model, the spun pile was only modeled from the top to the fixity point without the nonlinear soil spring. This simplification could save more time and memory files during cyclic analysis.

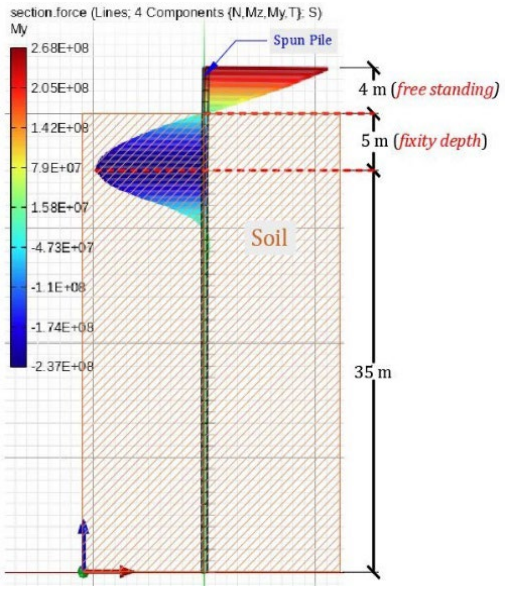

Figure 7. Fixity Depth of Spun Pile Idealization

Structural Idealization

The numerical structural span 5000 mm model SOP A has four bays in the y-axis direction and nine in the x-axis direction with span lengths of 2500 mm and 5000 mm, respectively. A total of 50 nodes were identified, including one control node, in the center to monitor the reaction of the structure, as illustrated in Figure 8. The numerical structural span 7500 mm model SOP B and SOP C has four bays in the y-axis direction and six in the x-axis direction with span lengths of 2500 mm and 7500 mm, respectively. The red line in Figure 9 shows the bays reinforced with 30 braced frames. A total of 35 nodes were identified, including one control node, in the center to monitor the reaction of the structure.

The SOP structures were modeled as fiber section elements in a three-dimensional model using STKO (OpenSees) software, as illustrated in Figure 8 and Figure 9. The mass is modeled as a lumped mass. The spun piles were assumed to be fixed in the lowest nodes and concrete mass was assigned to all top nodes of the spun pile: 214.96 kN, 267.43 kN, and 277.63 kN in the SOP-A, SOP-B, and SOP-C, respectively. The load is modeled as a lumped load applied to the nodes. The red line indicates the section reinforced with braced frames (double UNP profiles). The nine-meter-long piles were modeled using displacement-based beam-column elements, while pile elements were numerically modeled with fiber cross sections. The Gauss-Lobato integration method with five points was used to define the plastic-hinges of the pile. The beam element connecting the (inelastic) pile with the (elastic) element used a zero-length element with a rigid assumption.

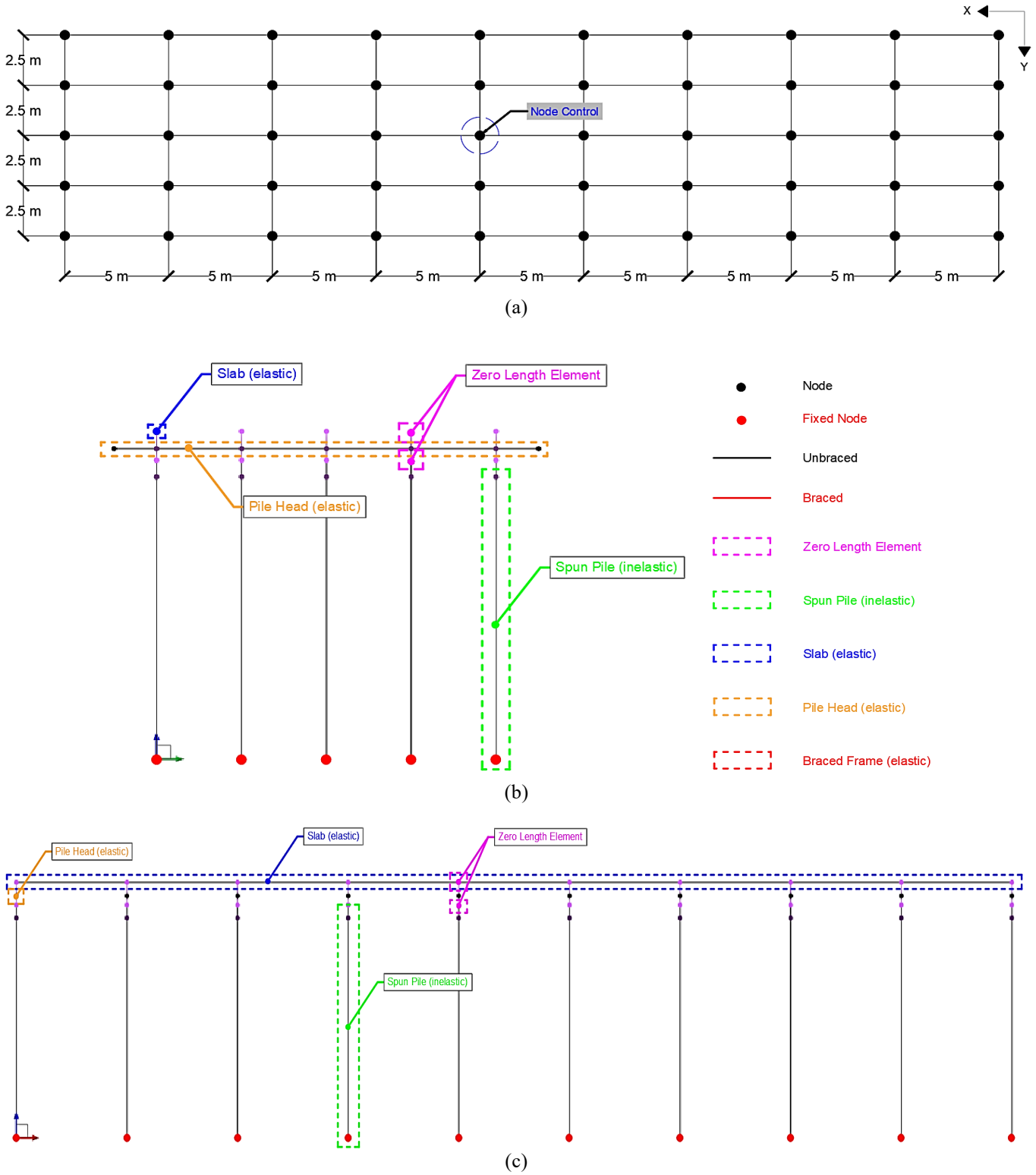

Figure 8. Structural Idealization of Slab-on-pile without Braced Frame: (a) Top View, (b) Front View, (c) Side View

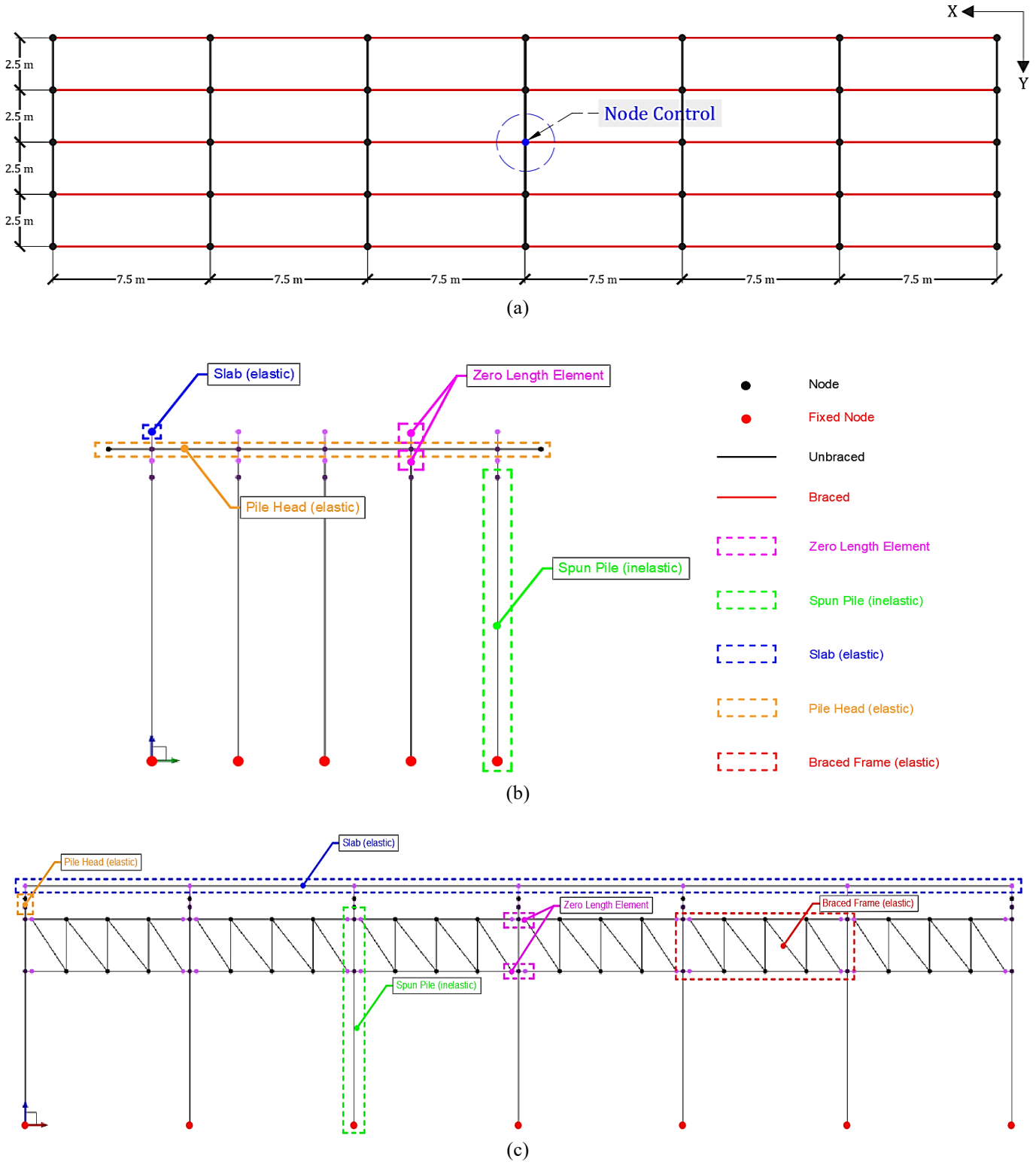

Figure 9. Structural Idealization of Slab-on-pile with Braced Frame: (a) Top View, (b) Front View, (c) Side View

Cyclic Analysis

The American Concrete Institute (ACI) provides guidance on moment frame acceptance based on structural testing for the design and evaluation of structures through document ACI 374-1-05 [15]. An important component of this document is the cyclic loading protocol, which provides insight into modeling the behavior of the structure. In this experimental study, the application of lateral cyclic loads followed a carefully designed loading protocol derived from the specifications outlined in ACI 374-1-05, a recognized standard in structural engineering. The complexity of this protocol, as shown in Figure 10, provides a systematic and controlled approach for applying varying lateral forces to the structure. At the core of this investigation is the drift ratio, a key metric defined as the ratio between lateral

displacement and shear span. This dynamic indicator offers insights into the structural response to applied lateral loads, capturing the deformation and displacement that occur during the experiment. Consequently, this study aimed to evaluate the behavior and bearing capacity of piles when faced with cyclic or vibration loads, due to earthquakes or other dynamic loads.

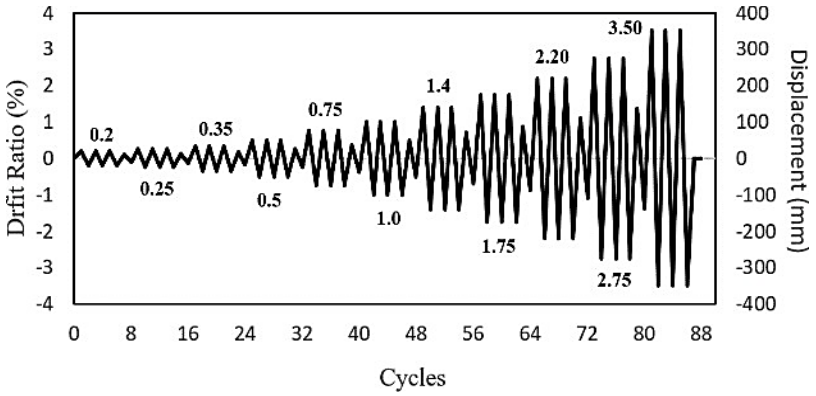

Figure 10. Cyclic Loading Protocol [15]

Energy Dissipation Capacity

Energy dissipation is essential in describing the performance characteristics of structures. This is evident through the dissipation of hysteresis energy (E_d) and equivalent viscous damping (h_e) during cyclic loading (Figure 11). Hysteresis energy dissipation represents the amount of damping in structural joints due to various mechanisms, such as material inelasticity. These parameters can be assessed using Equations (10) and (11).

$$Ed = \sum_{i=0}^{n} \frac{(F_{(i+1)}+F_i)}{2}(\Delta_{(i+1)} + \Delta_i) \quad (10)$$

$$h_e = \frac{1}{2\pi} \cdot \frac{S_{ABC}+S_{ADC}}{S_{\Delta OBE}+S_{\Delta ODF}} \quad (11)$$

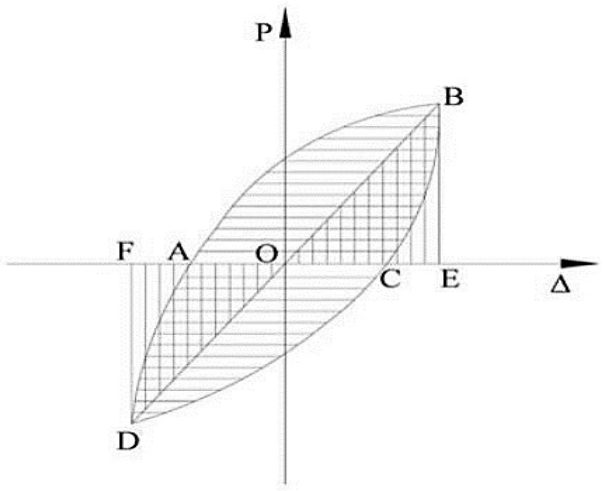

Figure 11. Definition of a Hysteretic Loop [21]

Results and Discussion

Modal Analysis

Modal analysis was performed to determine the natural behavior and fundamental period of the SOP structural model, as shown in Table 3. The modeling in this analysis used STKO software (OpenSees). The lowest fundamental period in the first mode occurred in SOP-A, serving as the stiffest structure, with a configuration of 50-spun pile. Meanwhile, the lowest fundamental period in the second mode occurred in SOP-C, with a configuration of 35-spun pile plus 30 braced frame, making the slab-on-pile structure stiffer by 1.58 - 1.78 times compared to others. This indicated that adding braced frames could increase the structure's stiffness.

Table 3. Natural Period of Slab-on-pile

Type	Mode	Natural Period (s)	Natural Frequency (H_z)
SOP-A	1	0.681	1.457
	2	0.610	1.637
SOP-B	1	0.774	1.291
	2	0.683	1.463
SOP-C	1	0.697	1.433
	2	0.386	2.586

Spun Pile Capacity

The pile capacity was analyzed based on lateral displacement, combined axial, moment forces (P-M interaction), and buckling. Figure 12 shows the P-M diagram of spun pile moment capacity interaction. All P-M responses of the SOP-A and SOP-C structures met the cross-section capacity requirements, except for the SOP-B. This was attributed to the 50-spun pile configuration of SOP-A, while SOP-B and SOP-C had 35-spun pile. In the SOP-C structure, 30-braced frame were added between the spun pile in the longitudinal direction of the structure. This additional braced frame made SOP-C fulfill all axial and moment force responses (P-M interaction), meeting the requirements of capacity. Consequently, it was concluded that the addition of 30-braced frame could reduce the use of piles by 15 pieces.

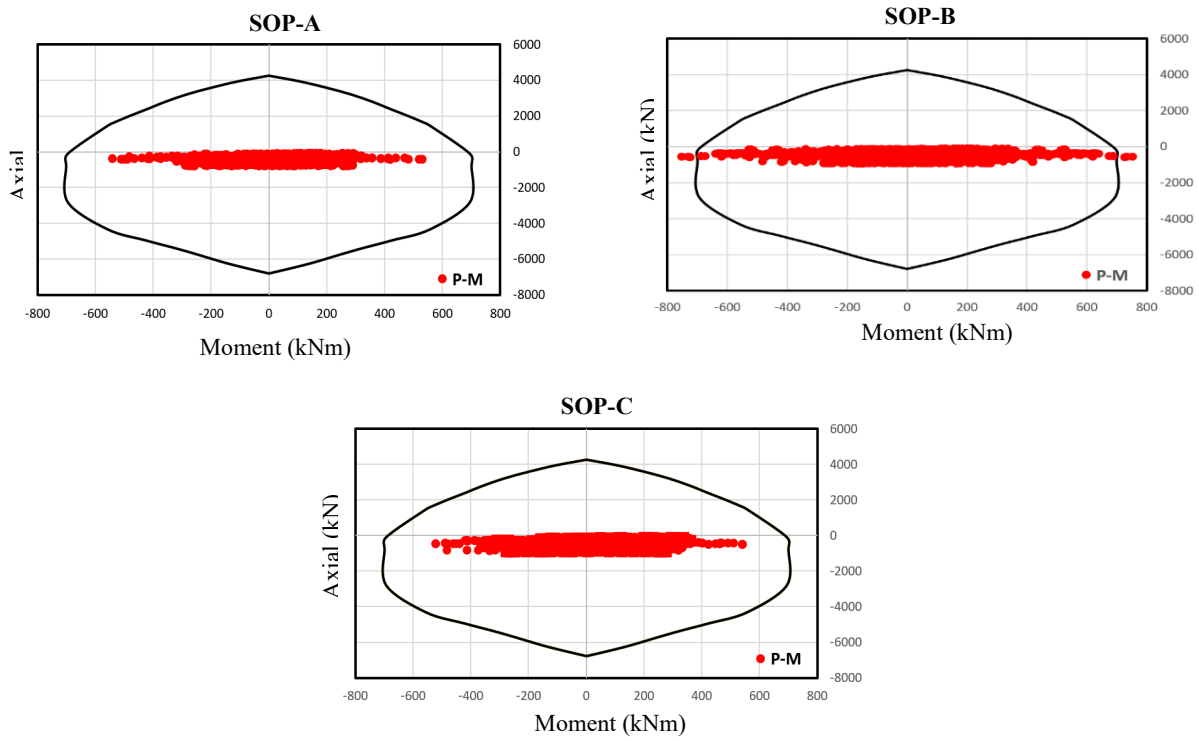

Figure 12. P-M Response of Spun Pile Element

Performance of The Structure

Figure 13 shows the results of the cyclic loading analysis in the longitudinal (X) and transverse (Y) directions. The hysteresis curve of the SOP-C structure in the longitudinal direction appeared greater than SOP-A and SOP-B. In SOP-C, the loading from the cyclic protocol was distributed to all 35-spun piles and partially dampened by the braced frame devices to obtain a greater curve and absorb more energy. In SOP-C the hysteretic loop has the greatest dissipation energy area, it shows the improved performance of the SOP structure with brace frame in support of cyclic loads. The increase in structural strength in the longitudinal direction of SOP-C was observed to increase significantly, while SOP-B has a smaller force. This indicated that the addition of braced frame devices could increase structural performance and structural strength. On the other hand, the hysteresis curve of the SOP-C structure in the transverse direction has the same appearance as SOP-B and has the lowest structural strength. In SOP-C, which has a configuration of 35 piles plus thirty braced frame is unable to equalize the structural strength of SOP-A with a configuration of 50 piles. This indicated that the configuration of the number of piles in the SOP structure greatly affects the structural performance and strength of the structure.

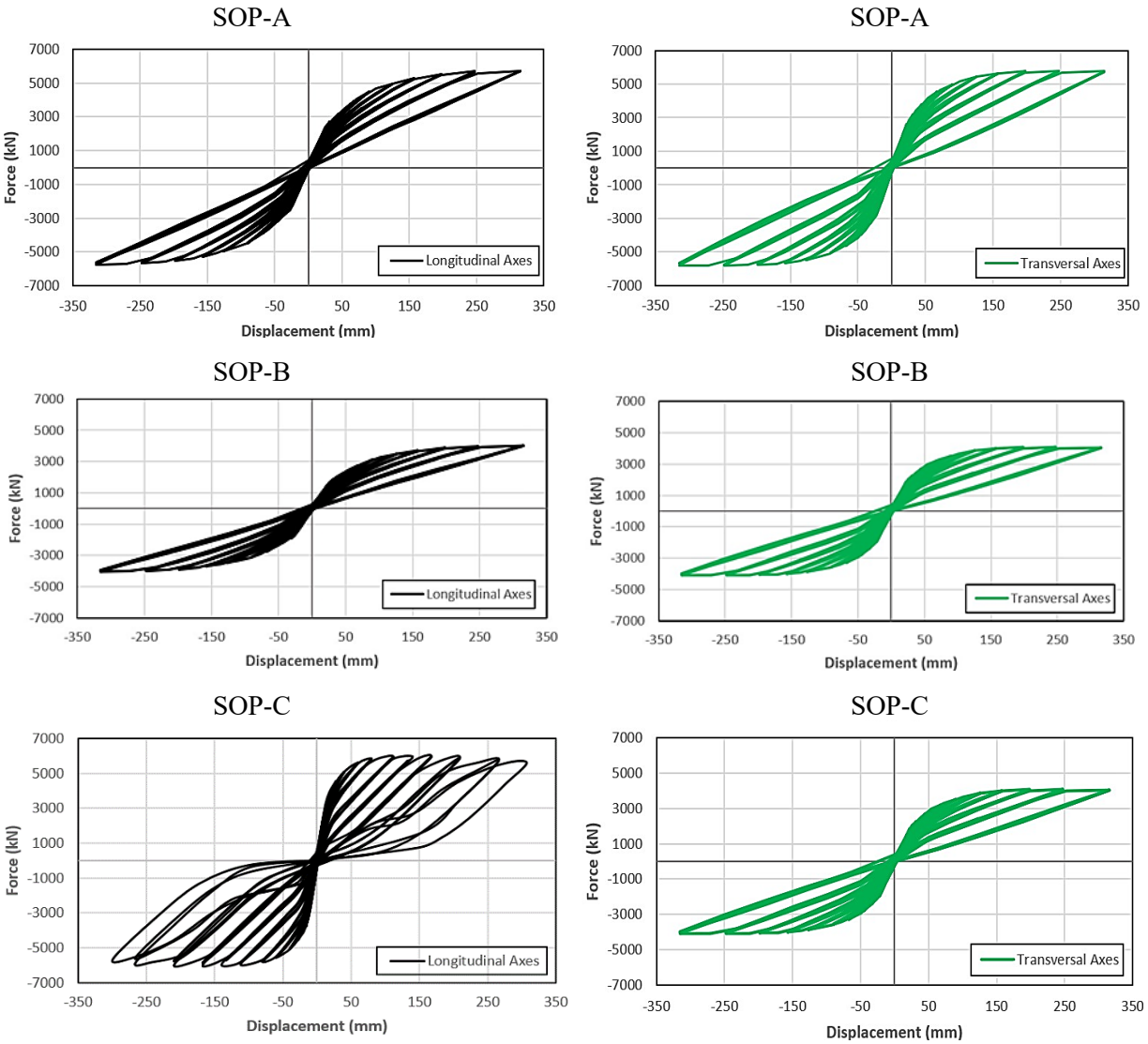

Figure 13. Hysteretic Curve of Slab-on-pile

A comparison of the hysteresis and viscous damping curves of the SOP structure with and without bracing is presented in Figure 14 and Figure 15. The addition of braced frames caused significant increase of energy dissipation of the slab-on-pile. The maximum force values that occurred in the SOP-A, SOP-B, and SOP-C structures were 5758.86 kN, 4035.78 kN, and 5990.50 kN, respectively. Furthermore, a significant increase was observed in the strength value of SOP-C against SOP-B by 32%, with the largest energy dissipation. This difference was observed when the three models reached the 19th cycle. Consequently, the energy dissipation capacity increased continuously as the cycle increased, in line with the viscous damping. The energy dissipation values for SOP-A, SOP-B, and SOP-C were found to be 2563 kNm, 1807 kNm, and 4226 kNm and the viscous damping values were 23%, 23%, and 38%, respectively. This indicated that the addition of braced frames to SOP-C increased the structural strength and dissipated energy by 5990.5 kN and 38%, respectively.

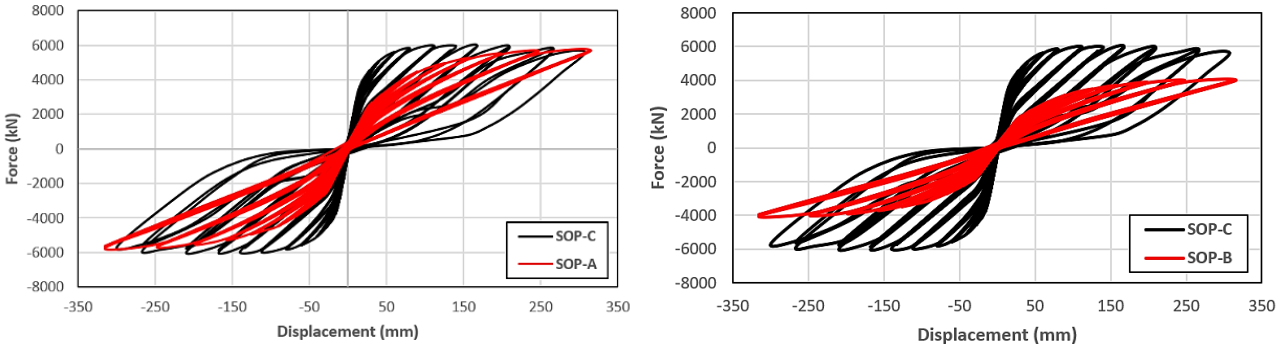

Figure 14. Comparison of Hysteresis Curves: SOP-C Structure with SOP-A and SOP B

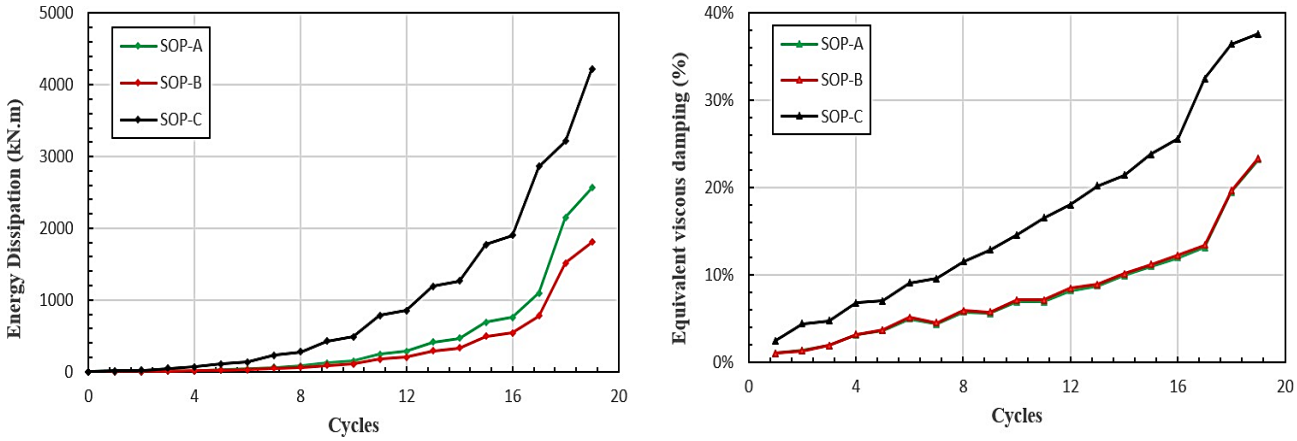

Figure 15. Comparison of Energy Dissipation and Equivalent Viscous Damping

Cost Analysis

The SOP optimization was carried out focusing on costs that were correlated with structural materials. Unit price analysis was conducted based on the Decree of the Mayor of South Sumatra Province No.452/KPTS/DPUPR/2022 [22] on the Standard Highest Unit Price of State Building for Fiscal Year 2023 and the brochure of PT Wijaya Karya (Beton) Tbk. Meanwhile, SOP-A and SOP-C models were compared to determine the more economical price. Based on the results, SOP-A structure with a 50-spun pile configuration showed good performance, fulfilling the structural capacity requirements. Similarly, SOP-C showed a good level of performance and fulfilled the structural capacity requirements. This indicated the need for a comparison between SOP-A and SOP-C to determine the efficiency in terms of cost. Based on the results of the cost analysis, the price difference between the SOP-A and SOP-C structures is Rp 613,276,820.49 consequently, the optimized SOP structure using an additional braced frame can minimize the cost of making the SOP structure by IDR 600 million.

Table 4. Cost-assumptions of SOP-A and SOP-C

Item SOP-A	Volume	Unit	Unit Price (Rp)	Price (Rp)
Spun pile Ø600 mm	50	pcs	61,309,270.76	3,065,463,537.79
Full Slab Precast				
erection	45	pcs	29,378,061.58	1,322,012,771.20
joint casting	77,44	m^3	2,114,756.00	166,090,002.09
Pile Head				
formwork	175	m^2	597,537.67	104,569,091.46
reinforcing work	2052,9	kg	85,519.75	175,559,829.64
casting work	61,3	m^3	2,100,900.50	128,680,155.63
			TOTAL	**4,962,375,387.82**
Spun pile Ø600 mm	35	pcs	61,309,270.76	2,145,824,476.45
Full Slab Precast				
erection	30	pcs	34,636,383.60	1,039,091,507.86
joint casting	50,06	m^3	2,489,125.00	
Pile Head				
formwork	122,50	m^2	597,537.67	73,198,364.02
reinforcing work	1437,00	kg	85,519.75	122,891,880.75
casting work	42,88	m^3	2,100,900.50	90,076,108.94
Braced Frame	35582,4	kg	20,543.93	732,002,284.00
			TOTAL	**4,349,098,567.33**

Conclusions

In this study successfully compared three models, namely SOP-A, SOP-B, and SOP-C, to determine the optimal slab-on-pile (SOP) design. Cyclic loading analysis and cost analysis were conducted as a basis for determining the optimal design. The results showed that SOP-C, the SOP that posses braced frame in longitudinal direction, was the most optimal design while SOP-B was the least. This indicated that the application of braced frame on slab on pile could increase the stability and performance of the structure. The SOP-C structure with the addition of braced frames had

a higher stiffness compared to the SOP-A and SOP-B structures, which were 1.58 - 1.78 times higher. Furthermore, it was discovered that the application of braced frames could reduce 15-spun pile and dissipate structural energy by 38%.

Acknowledgments

The authors are grateful to the Department of Civil and Environmental Engineering of Gadjah Mada University and PT Waskita Karya (Persero) Tbk for the support and contribution to this study.

References

1. Setiawan, A.F., Santoso, A.K., Darmawan, M.F., Adi, A.D., and Ismanti, S., Nonlinear Analysis for Investigating Seismic Performance of A Spun Pile-Column of Viaduct Structure, *Civil Engineering Journal*, *9*(7), 2023, pp. 1561-1578. Doi: 10.28991/Cej-2023-09-07-02.
2. WisDOT, Concrete Slab Structures: WisDOT Bridge Manual, July, 2023.
3. Yeung, A.T., Installation of Prestressed Spun High Strength Concrete Piles by Hydraulic Jacking, In *Proceedings of the HKIE Geotechnical Division 34th Annual Seminar*, 2014, pp. 109-115.
4. Kurniadi, A., Rosyidin, I.F., Indarto, H., and Atmono, I.D., Desain Struktur Slab on Pile, *Jurnal Karya Teknik Sipil*, *4*(4), 2015, pp. 57–68.
5. Wibawa, G.A., Sukrawa, M., and Sutarja, I., Efisiensi Perencanaan Jembatan Pile Slab dengan Bentang Bervariasi (Studi Kasus Jalan Tol Nusa Dua-Ngurah Rai-Benoa), *Jurnal Ilmiah Teknik Sipil*, *19*(1), 2015, pp. 54–62.
6. Walujodjati, E.W. and Cholik, Z., Pengaruh Pembesaran Dimensi Pile terhadap Kekuatan Struktur Pile Slab, *Siklus: Jurnal Teknik Sipil*, *8*(2), 2022, pp. 206–219.
7. Truman, K.Z. and Hoback, A.S., Optimization of Steel Piles under Rigid Slab Foundations using Optimality Criteria, *Structural Optimization*, *5*, 1992, pp. 30–36, 1992, DOI: 10.1007/Bf01744693.
8. Baroroh, I., *Desain Struktur dan Metode Pelaksanaan Piled Slab dengan Half Slab Precast dan Bracing pada Pile Proyek Relokasi Jalan Tol Porong-Gempol Paket 1 Sta 37+350 - 37+700 Sidoarjo - Jawa Timur*, Institut Teknologi Sepuluh Nopember Surabaya, 2018.
9. Türker, T. and Bayraktar, A., Experimental and Numerical Investigation of Brace Configuration Effects on Steel Structures, *Journal of Constructional Steel Research*, *67*(5), 2011, pp. 854–865. DOI: 10.1016/J.Jcsr.2010.12.008.
10. Kumar, M.S., Senthilkumar, R., and Sourabha. L., Seismic Performance of Special Concentric Steel Braced Frames, *Structures*, *20*, 2019, pp. 166–175. DOI: 10.1016/J.Istruc.2019.03.012.
11. Prayogo, D., Santoso, H., Budiman, F., and Jason, M., Layout, Topology, and Size Optimization of Steel Frame Design using Metaheuristic Algorithms: A Comparative Study, *Civil Engineering Dimension*, *24*(11), 2022, pp. 31–37. DOI: 10.9744/Ced.24.1.31-37.
12. Badan Standar Nasional Indonesia, *Beban Desain Minimum dan Kriteria Terkait untuk Bangunan Gedung dan Struktur Lain*, 2020.
13. Abebe, D.Y., Kim, J.W., Gwak, G., and Choi, J.H., Low-Cycled Hysteresis Characteristics of Circular Hollow Steel Damper Subjected to Inelastic Behavior, *International Journal of Steel Structures*, *19*(1), 2019, pp. 157–167, 2019. DOI: 10.1007/S13296-018-0097-8.
14. Badan Standar Nasional Indonesia, *Pembebanan untuk Jembatan SNI 1725-2016*, Jakarta, 2016.
15. American Concrete Institute, *ACI 374-1-05: Acceptance Criteria for Moment Frames based on Structural Testing and Commentary*, American Concrete Institute, 2005.
16. AASTHO, *Bridge Design Specifications*, September 2017. [Online]. Available: www.Transportation.Org.
17. Kent, D.C. and Park, R., Flexural Members with Confined Concrete, *ASCE Journal of the Structural Division*, 1971.
18. Quayyum, S., *Bond Behaviour of Fibre Reinforced Polymer (FRP) Rebars in Concrete*, Thesis, University of British Columbia, Canada, *2010*.
19. Mazzoni, S., Mckenna, F., Scott, M.H., and Fenves, G.L., *Opensees Command Language Manual*, 2006.
20. Irawan, C., Djamaluddin, R., Raka, I.G.P, Faimun, Suprobo, P., and Gambiro, Confinement Behavior of Spun Pile using Low Amount of Spiral Reinforcement - An Experimental Study, *International Journal on Advance Science, Engineering and Inf\ormation Technology*, *8*(2), 2018, pp. 501–507. DOI: 10.18517/Ijaseit.8.2.4343.
21. Yang, Z., Li, G., Wang, W., and Lv, Y., Study on the Flexural Performance of Prestressed High Strength Concrete Pile, *KSCE Journal of Civil Engineering*, *22*(10), 2018, pp. 4073–4082. DOI: 10.1007/S12205-018-1811-Y.

22. Keputusan Walikota Palembang, *Lampiran Keputusan Walikota Palembang Nomor 272/ Kpts/Bpkad/2022 Tentang Standar Harga Satuan Tahun 2023 di Lingkungan Pemerintah Kota Palembang*, 2023.